Proceedings of Heap Leach Mining Solutions, 2016
October 18-20, 2016, Lima, Peru
Published by InfoMine, © 2016 InfoMine, ISBN: 978-1-988185-03-3

Decoupling stresses from geosynthetic barrier systems, towards extended service life and safety

Laura Carbone, Huesker Synthetic GmbH, Germany
Morné Breytenbach, Huesker Synthetic GmbH, Germany
Fernando Ruiz, Huesker Limitada, Brazil

Abstract

Mine structures, particularly heap leach pads, usually incorporate geocomposite barrier systems. These barrier systems are exposed to extreme stresses for the duration of the structure's service life. Tensile stress imposed on geomembranes may cause premature stress cracking, which can lead to the economic and environmental failure of the barrier system and subsequently the heap leach facility. Various studies have shown that barrier systems should ideally be designed and also performed without stress. They are simply intended to act as barriers.

In this paper, two different scenarios of a typical liner system on a slope simulating the full and the partial mobilization of the interface friction angle are considered. The development of the acting forces in the geocomposite liners in the two scenarios is calculated and its effect on the stability and on the tensile load distribution between various geosynthetic barrier system components is analyzed. Finally, the influence of the deformations on the geomembrane's long-term serviceability is also discussed.

Introduction

Geomembrane liners have been used significantly in the mining industry since about 1970 for lining solution and evaporation ponds, tailings impoundments and heap leach pads (Breytenbach and Smith, 2006). Geomembranes, typically high-density polyethylene (HDPE), are included as barrier in lining systems (Rowe, 2005; Thusyanthan et al., 2007). As manufactured, HDPE is impermeable to liquid flow, and movement through intact HDPE is limited to diffusive processes, which are normally very slow. During its service life, a number of other factors including quality of installation, stresses caused by slope instability, contact with aggressive chemicals and the depletion of antioxidants may affect the properties of HDPE, which can give rise to defects or cause failure (Needham et al., 2006). These different degradation mechanisms may have synergistic effects that could accelerate the overall rate of HDPE geomembrane degradation (Rowe and Sangam, 2002).

The service life of a geomembrane liner can be defined as the range of time the liner continues to act as an effective hydraulic barrier for the purposes of the site under consideration (Needham et al., 2006). Thus, when a geomembrane is under stress at the same time as oxidation is occurring, the degradation process is more complex (Rowe and Sangam, 2002).

The design of lining systems on steep slopes is always a global challenge (Sabatini et al., 2002). The design should be environmentally acceptable for the duration of its intended service life. Typically, in the design, the two main states in which failure can occur are (Dookhi, 2014):

- Ultimate limit state where there is a complete loss of stability or function (example, slope failure),
- Serviceability limit state such that the function of a structure is impaired (example, stressing of a liner leading to increased permeability or to impaired stresses in slope).

The analysis of ultimate limit state (i.e., slope stability) is usually conducted by using the limit equilibrium concepts. Serviceability limit state relates to the stresses, strains and deformations, in the system and within defined liner components; this type of analysis requires usually more sophisticated analytical techniques such as finite difference and finite element formulations.

In this paper, two different scenarios of a typical liner system on slope are considered where a different in-situ mobilization of the interface shear strength is assumed. In fact, the interface friction angle is a very sensitive parameter and small changes in the boundary conditions can imply a loss in the shear strength (Carbone, 2014) that results in a decrease of the safety factor (Peng et al., 2016; Sabatini et al., 2002). The stability of the system in the two scenarios is analyzed by considering limit equilibrium analysis assuming the infinite slope approach. Whereas, the assessment of the tensile stress transferred to the different layers during operational conditions is calculated by applying a simple analytical model proposed by Liu and Gilbert (2003, 2005) that maintains strain compatibility and force equilibrium of the system.

Geosynthetic liner on slope: Main characteristics and assumptions

In this study a typical geocomposite lining system 30 m long, with a slope inclination equal to 13° is considered. The liner comprises the following interfaces from top to bottom (Figure 1):

- Granular soil layer
- Non-woven geotextile
- Double textured geomembrane
- Non-woven geotextile
- Base soil

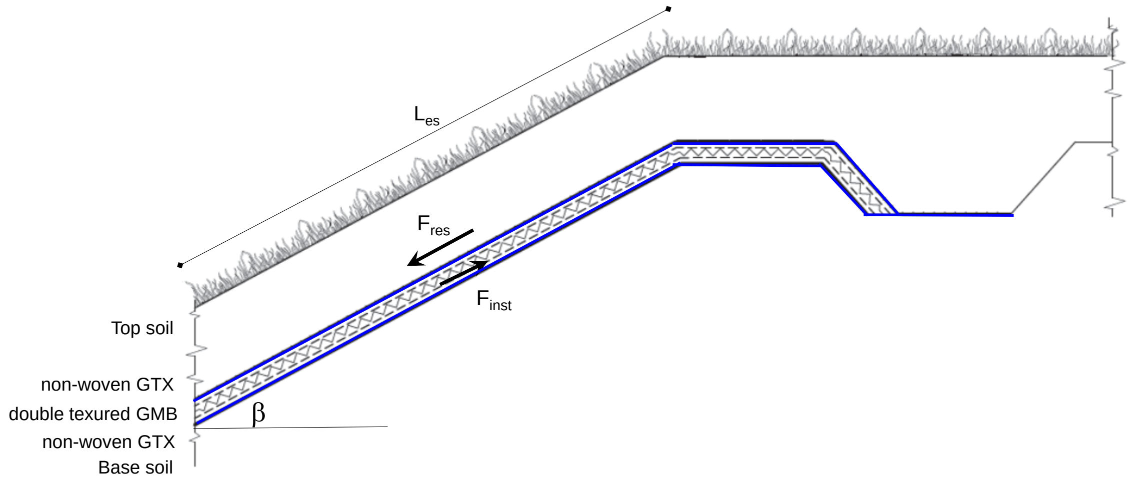

Figure 1: Scheme of the geocomposite liners considered in the study

The data for the textured HDPE geomembrane (GMB), for the non-woven geotextiles (GTX) and for the soils were acquired from literature (Frost and Lee, 2001; Liu and Gilbert, 2005; Peng et al., 2016) and shown in Table 1. In the system the two non-woven geotextiles are used as protection of the geomembrane against the top and the base soils respectively. According to Frost and Lee (2001) it is assumed that the thicker the geotextile, the higher the shear strength parameter. The GTX_1 of 543 gr/m^2 and the GTX_2 of 203 gr/m^2 are placed respectively on top and on bottom of the geomembrane.

The interface behavior was assured to be elastic-perfect plastic with a Mohr-Coulomb failure criterion.

Table 1: Characteristics of the geocomposite liners considered in the study

	Properties	Interface friction angles
Granular soil*	γ_{soil}= 18 kN/m^3 ϕ_{soil} = 32° t_{soil} = 0.7m K_c= 485 kN/m	$\phi_{soil/GTX}$ = 29°
Geotextile (GTX_1)	ρ=543 gr/m^2** $K_{t,GTX}$= 33.3 kN/m***	$\phi_{GTX1/GMB}$ = 21° (peak value) ** $\phi_{GTX1/GMB}$ = 12° (large displacement value) **
Geomembrane (GMB)	$K_{t,GMB}$= 380 kN/m***	$\phi_{GMB/GTX2}$= 19° (peak value) ** $\phi_{GMB/GTX2}$= 11° (large displacement value) **
Geotextile (GTX_2)* **	ρ=203 gr/m^2** $K_{t,GTX}$= 10.0 kN/m	$\phi_{GTX2/base}$= 25° ***

* Literature data from (Liu and Gilbert, 2005)

** Literature data from Frost and Lee, (2001) - see also Figure 3

*** Literature data taken from Peng et al., (2016)

Ultimate state: static stability analysis of the liner on slope

The analysis of slope stability of the geocomposite liner at the interface at the ultimate limit state is done by applying the limit equilibrium approach. The cover soil is considered as a rigid block resting on the on the geosynthetic package, where the interface between the soil and geosynthetic or between geosynthetics acts as a well-defined failure plane. Tangential stresses are mobilized along the geosynthetic interfaces and consequently, tensile forces are mobilized in the different geosynthetics (Carbone, 2014). Stability analysis is conducted by assuming an infinite slope approach, i.e., the cover soil is infinitely long such that the passive wedge is ignored. Stability under static loading can be maintained if the slope angle is less than the angle of friction between the most critical interfaces. The adhesion at the interface, seepage and external forces are not considered in this calculation.

Considering the normal and shear forces acting along the slope, and assuming a Mohr-Coulomb shear strength envelope, the factor of safety i.e., the ratio between the resisting and the driving forces can be expressed as:

$$FS = \frac{F_{res}}{F_{inst}} = \frac{W \cdot \cos\beta \cdot \tan\delta_{crit}}{W \cdot \sin\beta} = \frac{\tan\delta_{crit}}{\tan\beta} \tag{1}$$

where W is the top soil weight, β the slope inclination angle and δ_{crit} the critical interface friction angle, i.e., the interface that exhibits the lowest interface friction angle.

The resistance force (F_{res}) is considered as purely frictional and is calculated at the critical interface. Therefore, to run the calculation the proper evaluation of the interface friction angles is required. It is worth noting that the interface friction angle is a very sensitive parameter that changes according to the materials in contact and to the boundary conditions of the system (Carbone, 2014). Most of the geosynthetic-geosynthetic interfaces are usually characterized by strain-softening behavior (Blond and Elie, 2006; Carbone, 2014; Dookhi, 2014; Fox and Stark, 2004; Gallagher et al., 2016; Koerner, 2005; Sabatini et al., 2002) as shown in Figure 2. This implies that, in situ, if the residual interface friction angle is mobilized instead of the peak value, a loss in the interface shear strength can occur.

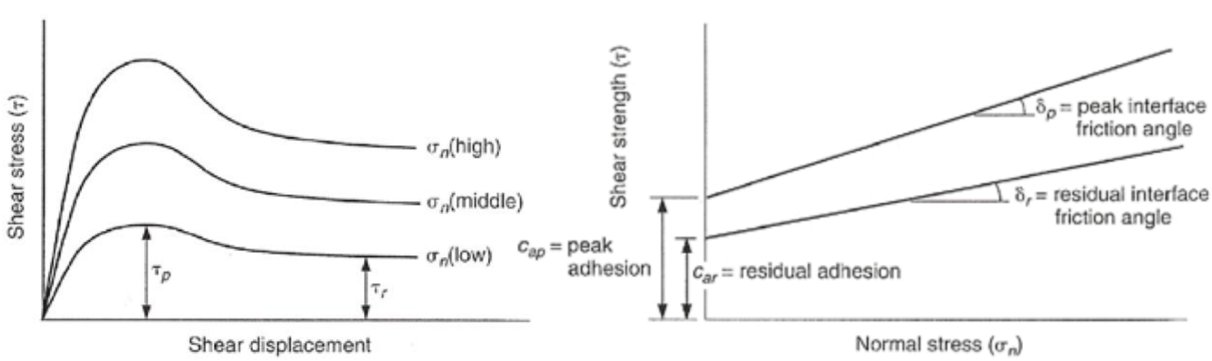

Figure 2: a) Direct shear test data; b) Mohr-Coulomb failure envelope (Koerner, 2005)

In the practice, the use of the peak, residual/large displacement or a combination of shear strength is still debated (Dookhi, 2014; Thiel, 2001). The residual shear strength is often much lower than the peak shear strength, especially when textured geomembranes are used (Carbone, 2014; Frost and Lee, 2001; Hebeler et al., 2005; Manheim et al., 2015). In this latter case, the general trend is principally attributed to the removal of micro-texture asperities of the geomembrane and to the wear of the material in contact (i.e., tearing of the filaments when a non-woven geotextile is the counter material) (Carbone, 2014; Frost and Lee, 2001).

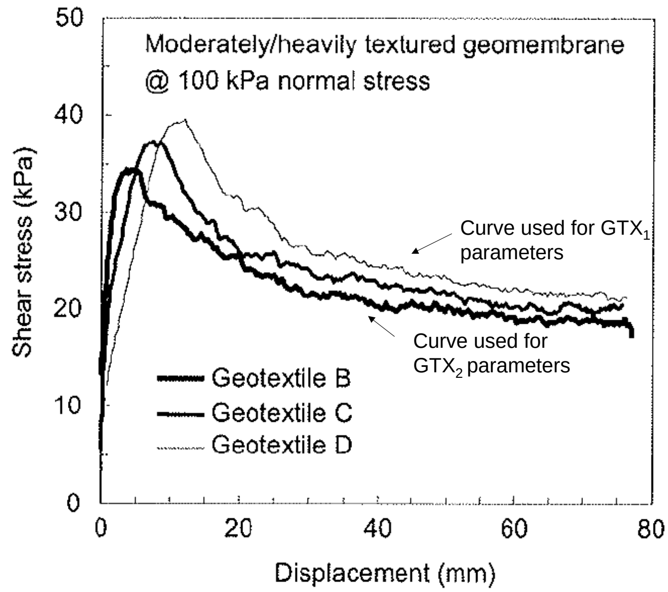

Figure 3: Typical stress –strain displacement curves of moderately/heavy textured geomembrane vs. non-woven geotextiles of different mass per unit area (modified from Frost and Lee, 2001)

Serviceability state: tensile forces on the lining system layers

Although the stability of the lining system is verified, the forces acting on the interfaces, in particular the tensile strength should be checked. In fact, the forces involved should be consistent with the allowable tensile strength of every geosynthetic (Carbone, 2014), especially when a geomembrane, that should not take any tensile strength, is part of the geocomposite system (Thusyanthan et al., 2007).

Since the calculation of tensile load transfer into the system is very complex, numerical analysis methods are usually employed. Liu and Gilbert (2005) proposed a set of graphical solutions based on an analytical model (Liu and Gilbert, 2003), in which force equilibrium and displacement compatibility between different components are satisfied. According to this model, if the applied driving force due to the weight of the cover soil (F_{inst}) exceeds the resisting force, the soil will compress at the toe of the slope producing a compression force in the soil (C_{soil}) and a tension force in the geosynthetic (T_{gs}). A net shear stress, ϕ_{net}, is induced along the geosynthetic layer and as well as the other forces acting on the system, are assumed to be uniformly distributed along the geosynthetic layer over the length of the top soil (L_{es}). Hence, these forces can be expressed as constant shear stresses. The model assumes that the soil and geosynthetics are two different columns. The soil column is fixed at the toe of the slope while the geosynthetic column is considered to be fixed at the anchor trench. It is also assumed that the slippage is not occurring at the interface between soil and geosynthetics so that the two columns strain equally (i.e., no relative displacement) and the deformation level mobilizes large displacement strength at the interfaces. The soil and geosynthetic layers are assumed to behave like elastic-plastic materials, with k_c representing the compressive stiffness of the soil and k_t representing the tensile stiffness of the geosynthetic. Non-linearity in these materials can be approximately accommodated by selecting secant stiffnesses that reflect the expected levels of deformation. For each layer the induced load is proportional to its tensile stiffness ($k_{t,GSY}$) relative to the total stiffness k_t.

The procedure followed to calculate the total tensile load T_{gs} transferred in the geosynthetics is summarized in Figure 4 while for further details see Liu and Gilbert (2005).

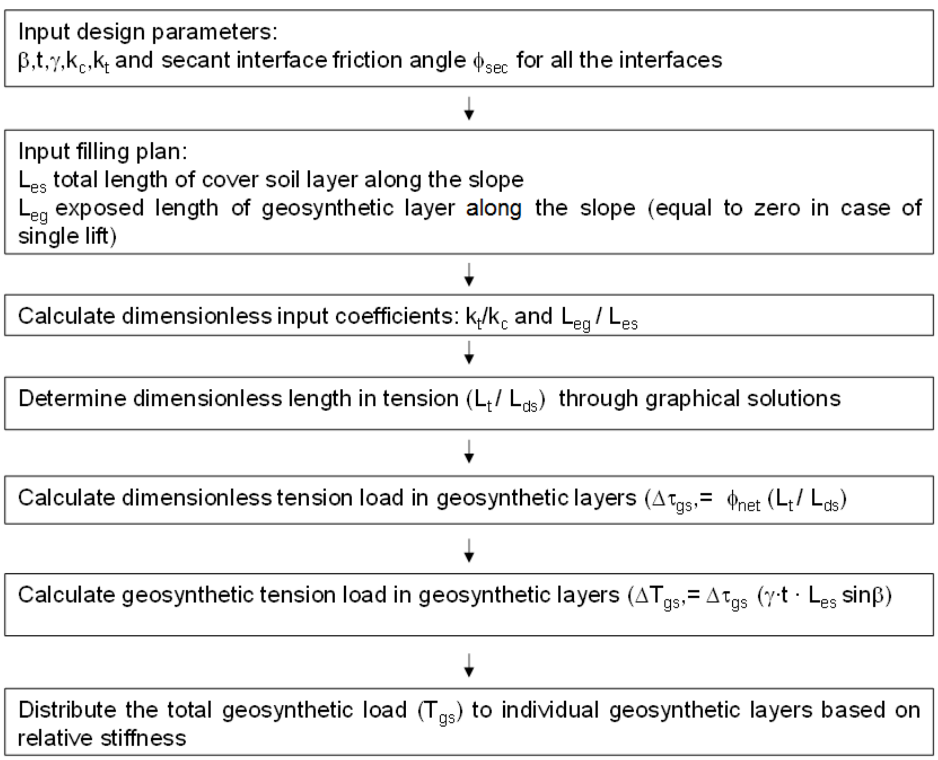

Figure 4: Procedure for estimating geosynthetic tension force (modified from Liu and Gilbert, 2005)

Results and discussion

The stability analysis of the geocomposite slope was carried out applying Equation (1) using the input values in Table 1. As can be noted, the critical interface friction angle is the one corresponding to the GMB-GTX_2 interface. The resisting force is therefore calculated according to the mechanical properties at this interface. In the calculation, two main scenarios were considered:

- design with the mobilization of the peak interface friction angle (scenario A);
- design with the mobilization of the large displacement interface friction angle (scenario B).

Table 2 shows the results of the stability analysis of the slope in the two considered scenarios. It can be noted that if progressive failure occurs, large displacement instead of the peak interface friction angle is mobilized. In this case, the loss in the interface shear strength at the critical interface is of about 43%. Consequently, the factor of safety (FS) drops down from 1.5 to 0.8 and the slope stability is no more verified. It is worth nothing that the residual interface friction angle is generally mobilized for values of displacements of about 80 mm for interfaces including non-woven geotextiles – slightly/moderately/heavily textured geomembranes (Frost and Lee, 2001; Stark et al. 1996). Therefore, if large displacement shear strength is mobilized, for example as a consequence of installation damage, the loss in shear strength should be taken by a geosynthetic of reinforcement.

Generally speaking if all of the interface shear strengths are greater than the slope angle, stability is achieved and it is assumed that the only deformation involved is a small amount to achieve elastic equilibrium (Dookhi, 2014; Peng et al., 2016). However, if any interface shear strengths are lower than the slope angle, wide-width tensile stresses are induced into the overlying geosynthetics (Thusyanthan et al., 2007). In this case, the analytical model by Liu and Gilbert (2005) was applied to calculate the tensile force that may possibly be transferred to the geosynthetic layers of the system in case a loss in shear strength from peak to large displacement values occurs (scenario B).

Table 2: Geocomposite liner on slope results at the ultimate state (stability analysis) and during serviceability state (tensile load transfer to the geosynthetic layers)

	ULTIMATE STATE		SERVICEABILITY STATE	
Deformation at the critical interface	Resisting force R_d (kN/m)	Safety factor (FS)	Model parameters	Tensile load carried by every single layer
Small displacement (scenario A)	126.8	1.5	–	–
Large displacement (scenario B)	71.6	0.8	ϕ_{net}=0.16 ΔT_{gs}= 6.3 kN/m	GTX: 8 % GMB: 92%

The model results are shown in Table 2. The use of a textured geomembrane allows a better interaction and therefore enables to reach higher slope inclinations. However, if the actual interface friction angle decreases with respect to the design value (peak value) and it is lower than the slope inclination angle, the geomembrane will be subjected to tensile load and will carry the majority (92%) of that tensile load, ΔT_{gs} (scenario B).

If the acting stresses are high, ductile tensile failure of the geomembrane can occur (Needham et al., 2006). If the tensile load taken by the geomembrane is lower than its ultimate tensile strength, creep phenomena can take place. This may affect the mechanical properties of the material and consequently its long term behavior.

In situ, the behavior of geomembrane can be influenced by different mechanisms such as swelling, UV degradation, degradation by extraction, biological degradation, and oxidative degradation (Rowe, 2005) as well as by other physical damages defects or holes due to stress cracking or as a result of a poor quality of installation. Furthermore, these different degradation mechanisms may have synergistic effects that could accelerate the overall rate of HDPE geomembrane degradation.

Figure 5 schematizes the three conceptual stages of HDPE geomembrane chemical aging. It can be noted that after antioxidants depletion and polymer degradation phase (stages A and B), chemical and physical degradation are acting together during Stage C. As stated by Rowe and Sangam (2002), a direct consequence of the degradation that occurs during Stage C is the decrease of both stress and strain at break while tensile modulus and yield stress increase. As the degradation progresses further, the geomembrane will become increasingly brittle and the tensile properties change to the point that cracking occurs in stressed areas. Once sufficient cracks have developed to significantly increase the flow through the geomembrane, the geomembrane may be considered to have reached the end of the so-called ''service life''.

This can have a more significant effect in heap leaching where a combination of extreme pressures and high moisture conditions are present (Breytenbach and Smith, 2006).

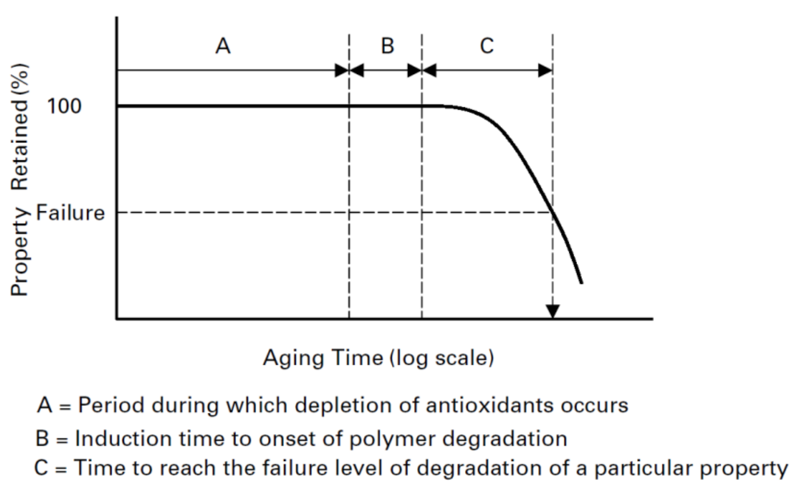

Figure 5: The three conceptual stages in chemical aging of HDPE geomembranes (adopted by Rowe and Sangam, (2002) modified from Hsuan and Koerner, 1998)

Conclusion

With the increased frequency of the utilization of geomembranes with regards to the lining system of critical structures such as Heap Leach facilities, so too does the understanding of the factors which impact the service life of these barriers increase. It is fundamentally important that a geomembrane barrier retains its intended key function, that of an environmental barrier, any stresses which could possibly be transferred to the geomembrane should be avoided and diverted to material solutions which are intended and designed for carrying loads, constantly.

Towards this end, in this study two different scenarios of a typical liner system on slope are considered. The stability of the system was analyzed by taking into account the occurrence of a progressive failure i.e., peak and large displacement interface shear strength mobilization. The results show that in this case the factor of safety (FS) drops dramatically down from 1.5 to 0.8 and the slope stability is no more verified. Furthermore, the tensile force that might be transferred to the system is calculated by applying the analytical model proposed by Liu and Gilbert (2003, 2005) that maintains strain compatibility and force equilibrium of the system. The calculation shows that in case of progressive failure, the geomembrane will take the major part of the load that implies that it is acting as non-intentional reinforcement.

The tensile force acting together with other degradation mechanisms can lead to a reduction in the service life of the geomembrane.

Therefore, the means for decoupling loads from barrier systems should be evaluated in every case and where appropriate applied to ensure the responsible design and operation of lined structures these solutions.

References

Blond, E. and Elie, G. 2006. Interface shear-strength properties of textured polyethylene geomembranes, in Sea to Sky Geotechnique 2006: 898-904.

Breytenbach, A.J. and Smith, M.E. 2006. Overview of geomembrane history in the mining industry, in Proceedings of 8th bi-annual meeting of the International Geosynthetics Society (8IGS), Japan, September 2006.

Carbone, L. 2014. Interface behavior of geosynthetics in landfill cover systems under static and seismic loading conditions, Ph.D. Dissertation. Mediterranea University of Reggio Calabria and University of Grenoble, 215 pp.

Dookhi A.S. 2014. Inversely unstable – the lining of steep landfill slopes in South Africa, in Proceedings of the 20th WasteCon Conference 6-10 October 2014, Somerset West, Cape Town: 174-188.

Fox, P.J. and Stark, T.D. 2004. State of the art report: GCL shear strength and its measurement, Geosynthetics International, 11(3): 141-175.

Frost, J.D. and Lee, S.W. 2001. Microscale study of geomembrane - geotextile interactions. Geosynthetics International 8: 577-597.

Gallagher, E.M., Tonks, D.M., Shevelan, J. and Belton, A.R. 2016. Investigations of geomembrane integrity within a 25-year old landfill capping, Geotextiles and Geomembranes, retrieved from http://dx.doi.org/10.1016/j.geotexmem.2016.05.011

Hebeler, G., Frost, J. and Myers, A. 2005. Quantifying hook and loop interaction in textured geomembrane-geotextile systems, Geotextiles and Geomembranes 23: 77-105.

Hsuan, Y.G. and Koerner, R.M. 1998. Antioxidant depletion lifetime in high density polyethylene geomembranes, Journal of Geotechnical and Geoenvironmental Engineering ASCE: 532–541.

Liu, C.-N. and Gilbert, R.B. 2003. Simplified method for estimating geosynthetic loads in landfill liner side slopes during filling. Geosynthetics International, 10(1): 24-33.

Liu, C-N. and Gilbert, R.B. 2005. Graphical solutions for estimating geosynthetic loads in geosynthetic–soil layered systems on slopes, Geosynthetics International, 12(4): 208-214.

Manheim, D.C., Yesiller, N., Hanson, J.L., Gourc, J.P., Carbone, L., Moraci, N., Carrubba, P. and Pavanello, P. 2015. Investigation of post-shear surface texture characteristics of geomembranes, Geosynthetics 2015 February 15-18, Portland, Oregon.

Koerner, R.M. 2005. Designing with geosynthetics, Fifth Edition, Pearson Prentice Hall, NJ, USA.

Needham, A.D., Smith, J.W.N., and Gallagher, E.M.G. 2006. The service life of polyethylene geomembrane barriers, Engineering Geology, 85: 82–90.

Peng, R., Hou, Y., Zhan, L. and Yao, Y. 2016. Back-analyses of landfill instability induced by high water level: Case study of Shenzhen landfill, in International Journal of Environmental Research and Public Health, 13: 126.

Rowe, R.K. 2005. Long-term performance of contaminant barrier systems, Geotechnique, 55(9): 631-678.

Rowe, R.K. and Sangam, H.P. 2002. Durability of HDPE geomembranes, Geotextiles and Geomembranes, 20: 77-95.

Sabatini, P.J., Griffin L.M., Bonaparte, R., Espinoza R.D. and Giroud, J.P. 2002. Reliability of state of practice for selection of shear strength parameters for waste containment system stability analyses, Geotextiles and Geomembranes, 20: 241-262.

Stark, T., Williamson, T. and Eid, H. 1996. HDPE geomembrane/geotextile interface shear strength, Journal of Geotechnical Engineering, ASCE 122(3): 197-203.

Thiel, R. 2001. Peak vs. residual shear strength for bottom liner stability analyses, Proceedings of the GRI-15 Conference, Houston: 40-70.

Thusyanthan, N.I., Madabhushi, S.P.G. and Singh, S. 2007. Tension in geomembranes on landfill slopes under static and earthquake loading – centrifuge study, Geotextiles and Geomembranes, 25: 78-95.